Brain Structure and Function (2019) 224:3133–3144
https://doi.org/10.1007/s00429-019-01953-2

ORIGINAL ARTICLE

Segregated precuneus network and default mode network in naturalistic imaging

ZhengZheng Deng[1,2,3] · JinFeng Wu[1,2] · JiaQi Gao[1,2] · Yang Hu[3,4] · YiWen Zhang[3,4] · YinShan Wang[1,2] · HaoMing Dong[1,2] · Zhi Yang[3,4] · XiNian Zuo[1,2]

Received: 5 January 2019 / Accepted: 31 August 2019 / Published online: 12 September 2019

Abstract

A resting-state network centered at the precuneus has been recently proposed as a precuneus network (PCUN) or "parietal memory network". Due to its spatial adjacency and overlapping with the default mode network (DMN), it is still not consensus to consider PCUN and DMN separately. Whether considering PCUN and DMN as different networks is a critical question that influences our understanding of brain functions and impairments. Previous resting-state studies using multiple methodologies have demonstrated a robust separation of the two networks. However, since there is no gold standard in justifying the functional difference between the networks in resting-state, we still lack of biological evidence to directly support the separation of the two networks. This study compared the responses and functional couplings of PCUN and DMN when participants were watching a movie and examined how the continuity of the movie context modulated the response of the networks. We identified PCUN and DMN in resting-state fMRI of 48 healthy subjects. The networks' response to a context-rich video and its context-shuffled version was characterized using the variance of temporal fluctuations and functional connectivity metrics. The results showed that (1) scrambling the contextual information altered the fluctuation level of DMN and PCUN in reversed ways; (2) compared to DMN, the FC within PCUN showed significantly higher sensitivity to the contextual continuity; (3) PCUN exhibited a significantly stronger functional network connectivity with the primary visual regions than DMN. These findings provide evidence for the distinct functional roles of PCUN and DMN in processing context-rich information and call for separately considering the functions and impairments of these networks in resting-state studies.

Keywords Resting-state networks · Default mode network · Precuneus network · Natural viewing · Functional connectivity

Introduction

Resting-state networks (RSNs) characterize large-scale brain networks and have been widely investigated in resting-state fMRI (Biswal et al. 1995; Fox et al. 2005; Golland et al. 2007). Among the commonly investigated RSNs, a "Precuneus Network"(PCUN), or the so-called "Parietal Memory Network" (Gilmore et al. 2015), has recently been argued as a functional independent RSN from the well-known default mode network (DMN), although it is spatially adjacent and even overlapping with the DMN in some regions (Hu et al. 2016; Yang et al. 2014). The proposed network conforms to the existing RSN atlas. For instance, the regions of PCUN are not assigned to DMN in Yeo's RSN templates (Yeo et al. 2011). Previous studies have indicated the differences between these two RSNs (Power et al. 2011; Shirer et al. 2012; Smith et al. 2013; Yeo et al. 2011). There is also evidence that the regions of PCUN have a different life-span

✉ Zhi Yang
yangz@smhc.org.cn

1 Key Laboratory of Behavioral Sciences, Research Center for Lifespan Development of Mind and Brain, Institute of Psychology, Chinese Academy of Sciences, Beijing, China

2 Department of Psychology, University of Chinese Academy of Sciences, Beijing, China

3 Shanghai Key Laboratory of Psychotic Disorders, Shanghai Mental Health Center, Shanghai Jiao Tong University School of Medicine, 600 South Wanping Rd, Shanghai 200030, China

4 Brain Science and Technology Research Center, Shanghai Jiao Tong University, Shanghai, China

development trajectory (Yang et al. 2014) and can be separated from the DMN in resting-state fMRI data with multiple methodologies (Hu et al. 2016; Yeo et al. 2011), suggesting that the PCUN may play a different functional role than the DMN. However, since there is no gold standard in resting-state data to justify the validity of the parcellation of RSNs, the separation of PCUN and DMN has not reached a consensus in most resting-state studies. Clarifying this issue is important because the segregation between the PCUN and DMN is not only a question of how to parcel the brain networks but also an issue related to our understanding of the pathophysiology of mental disorders. Confusing the two RSNs may bias our understandings of brain function (Jones et al. 2016; Manoliu et al. 2014).

The PCUN consists of the precuneus, middle cingulate cortex, posterior inferior parietal lobule, and dorsal angular gyri. The DMN has been related to the internally directed cognitive processes (Andrews-Hanna et al. 2010; Buckner et al. 2008; Laird et al. 2011) and is sensitive to mental state changes or diseases (Greicius et al. 2004; Menon 2011; Padmanabhan et al. 2017), whereas the regions of PCUN have been primarily associated with memory functions and detection of novelty (Chen et al. 2017; Gilmore et al. 2019; Gilmore et al. 2015; McDermott et al. 2017). However, whether these regions should be attributed to PCUN and whether the PCUN should be deemed as a separated network in the resting-state study have not been clarified.

In recent years, a paradigm that uses natural stimuli, such as commercial movies, oral speech, or photos of daily life, has become popular (Huth et al. 2016; Peelen et al. 2009; Vanderwal et al. 2017; Vanderwal et al. 2015; Wilson et al. 2008). In contrast to repetitive task paradigms such as the go/no-go paradigm or the N-back paradigm, the natural stimuli paradigm presents multiple stimuli simultaneously to guide the subjects into a 'natural mental state', which is relatively close to the mental state people experience during real life. The natural stimuli paradigm can synchronize brain activity across subjects (Hasson et al. 2004; Lankinen et al. 2014; Simony et al. 2016) to control the physiological noise (Vanderwal et al. 2015). The natural stimuli paradigm, therefore, provides an alternative way to reveal the functional organization of the human brain.

In this study, we examined the functional roles of the two RSNs, PCUN and DMN, in the real-life context. It would be more convincing to deem the PCUN and DMN as different RSNs if they behaved differently in real-life information processing. As reviewed above, the core regions of PCUN have been related to the formation of memory, personal experience of novelty; while, DMN is related to the spontaneous internally directed thought. Watching a movie with intact stories would guide subjects to immersively comprehend the story. During continuously comprehending the story, subjects occasionally need to recall previous stories or feel familiar, so the PCUN's representative time series would be fluctuating. DMN would be consistently activated as the subjects were continuously relating the story to themselves, resulting in the stable representative time series of DMN. Watching a storyline-scrambled movie would suppress the representative time series of DMN because attention would be directed to remember, recall and infer the story. In such condition, PCUN would be stably activated since it consistently takes part in the memory-retrieval process. We hypothesized that (1) during watching a movie presenting intact storyline, DMN would be stably active as the participants are devoting themselves to the story; DMN's representative time series would be suppressed by the increased cognitive load when viewing the storyline-scrambled movie, and (2) compared with when watching a movie with intact story, the PCUN would be more consistently activated to handle the memory-retrieval and old/new comparison processes during watching the storyline-scrambled movie. To examine these hypotheses, we characterized and compared the representative time series fluctuations of the PCUN and DMN when subjects watched a movie and its temporally scrambled version. The two conditions shared identical visual properties but were different in whether they conveyed continuous, comprehensible stories. To reveal the difference in responding representative time series patterns between the PCUN and DMN, we compared the variance of their representative time series in the two conditions. A visual network, which is commonly observed in the medial visual cortex (Calhoun et al. 2008a; Smith et al. 2009; Van Den Heuvel et al. 2009), was used as a reference network. This network also showed high inter-subject consistency when being examined in the naturalistic paradigm (Hasson et al. 2004). Besides, the function of this network is the most relevant to neural processing of the visual contents, and the visual contents of the two movie conditions were well matched. We assumed that the responses of the medial visual network (mV) to different movie conditions were the most similar among all the RSNs. The functional coupling among the PCUN, the DMN, and the mV was also compared.

Materials and methods

Subjects

The research was approved by the ethics committee of the Institute of Psychology, Chinese Academy of Science. Forty-eight subjects (23 males, 25 females, mean age 25.6 ± 4.9) were recruited from the local community. A phone screening interview assessing the medical history, the family medical history, and other relevant neuropsychological states of the subjects was conducted before they participated in the study. Exclusion criteria included (1) the presence of neurological

or psychiatric conditions; (2) a history of drug or alcohol dependence; and (3) a history of MRI-incompatible conditions. All subjects signed the informed consent before participating in the experiment.

Experimental design

The experiment includes one resting-state and two movie-watching conditions. To avoid introducing cognitive content or emotional states into the resting-state condition, the resting-state scans were always conducted before the movie-watching scans and right after the T1-weighted anatomical scans. Two natural movie clips were presented to the subjects in the movie-watching conditions. One movie clip consisted of 6 public interest advertisements (called a normal movie). As depicted in Table 1, the length of the advertisements ranged from 30″ to 2′01″, and the total length of the video clip was 7′49″. The other movie clip was a shuffled version of the first clip. Each advertisement was temporally cut into 1-s segments, and the segments were randomly shuffled and concatenated to generate the scrambled version. The 6 scrambled advertisements were then concatenated to generate the random movie. The presentation order of the two movie clips was counterbalanced among subjects.

Data acquisition

All images were collected using a 3T GE MR750 MRI scanner at the Institute of Psychology, Chinese Academy of Science. A high-resolution structural scan was acquired using a T1-weighted sequence (matrix = 256 × 256, slice thickness = 1.0 mm, no gap between slices). The resting-state scan was acquired with an echo-planar imaging (EPI) sequence (42 axial interleaved slices, acquisition direction was from bottom to top, FOV = 220 mm, matrix = 64 × 64, slice thickness/gap = 3.5/0.5 mm, TR/TE = 2000/30 ms, flip angle = 90°, 300 volumes in total). During the resting-state scan, the subjects were instructed to lie in the scanner and look at the white fixation, which was placed in the center of the black background. Functional scans for movie-watching conditions were also acquired with an EPI sequence (42 axial interleaved slices, from bottom to top, FOV = 220 mm, matrix size = 64 × 64, slice thickness = 3.0 mm, no gap, TR/TE = 2000/30 ms, flip angle = 70°, 236 volumes in total). During the movie-watching scans, the subjects were instructed to watch the movie as in daily life.

Preprocessing

The data preprocessing for T1 images includes several generic steps conducted by the connectome computation system (CCS) (Xu et al. 2015). The structural images were first preprocessed by the Volbrain (http://volbrain.upv.es) (Manjón and Coupé 2016) to extract the brain tissue. Then, the tissue segmentation of the structural image was performed using FreeSurfer (Fischl 2012). All T1 images were normalized to MNI152 space using advanced normalization tools (ANTs) (Avants et al. 2011).

For the fMRI data, the preprocessing steps include: (1) dropping the first 5 TRs for the equilibrium of the magnetic field; (2) despiking; (3) slice timing; (4) reorienting the image into RPI orientation; (5) correcting head motion to the average time series; (6) removing the skull; (7) grand mean scaling to 10,000; (8) segmenting the white matter (WM) and cerebral–spinal fluid (CSF); (9) estimating the head motion parameters; (10) extracting the average WM signal and CSF signal by applying the tissue mask from step 9; (11) removing the contribution of head motion, WM and CSF to the BOLD signals by implying a regression model; (12) band-pass filtering with 0.01–0.1 Hz; (13) detrending; and (14) 6-mm spatial smoothing.

Independent component analysis

The preprocessed resting-state fMRI dataset was first decomposed into independent components (ICs) using the MELODIC module in FSL (Beckmann and Smith 2004). To minimize the influence introduced by the preprocessing steps that may cause signal mixing across voxels, the preprocessing for the resting-state dataset only included the steps from (1) to (7) as well as the 0.01–0.1-Hz band-pass filtering. Previous study showed that concatenating datasets

Table 1 A summary of the advertisements included in the natural movie stimuli

Order	Name	Duration in second	Description
1	Animal Humane Society	30	Cute cats in an animal welfare facility
2	The World is Where We Live	52	Side-by-side clips of the human world and the animal world to show the connection between humans and wildlife
3	A Love Story in Milk	121	A love story between two milk bottles
4	Water ink	87	Painting with water and black ink
5	50 Years of Flower Power	112	A story about the Struggle for Human Rights in the last 50 years
6	You can help save the Cerrado	65	Fingertut demonstrating the wildlife

from different subjects and run group-level ICA could split the DMN into an anterior and posterior component (Hu et al. 2016). The PCUN could be obtained in such an approach though. Thus, the decomposition step was run separately over the resting-state fMRI data for each subject. The numbers of ICs were automatically estimated by MELODIC and therefore varied across subjects. We used a data-driven tool, gRAICAR, to align the ICs among subjects. Briefly, gRAICAR (Yang et al. 2008; Yang et al. 2012) assessed the mutual information between all possible pairs of ICs among subjects and assigned all ICs to several groups according to the similarity. A spatial map was generated for each group of ICs by weighted averaging all ICs within that group. This map was thereby called an aligned component (AC). Subsequently, all ACs were ranked according to their consistency across subjects.

Identify the PCUN and DMN

The DMN and PCUN were selected manually according to the following rules: (1) The AC is similar to the spatial pattern that was discovered in previous studies. (2) The AC representing the DMN/PCUN has a relatively high intersubject consistency. (3) The activating region of the AC is located in gray matter and covers the anchor regions of the DMN/PCUN. According to previous studies, the anchor regions of the DMN include the posterior cingulate cortex (PCC), lateral parietal cortex (LPC), and medial prefrontal cortex (MPFC) (Calhoun et al. 2008a, b; Raichle 2015). The anchor regions of the PCUN included the PCU, mid-cingulate cortex (MCC), posterior inferior parietal lobule (pIPL), and dorsal angular gyrus (dAG) (Gilmore et al. 2015).

Representative time series of the PCUN and DMN in movie conditions

Briefly, the network representative time series of the PCUN and DMN in the normal and random movie conditions were derived using a regression model, as implemented in the dual-regression approach (Beckmann et al. 2009; Zuo et al. 2010), the detail is shown below. The previously matched IC maps in the resting-state fMRI data were converted into *Z* scores and were spatially transformed into the native space of the movie-watching data using ANTs. The transformed IC maps were used as regressors to interpret the preprocessed fMRI data in movie-watching conditions. By including all the ICs decomposed by ICA into the regression model, the contribution of each component could be modeled, including those representing irrelevant signals (e.g., signals from white matter and cerebrospinal fluid). This step resulted in a set of representative time series. The derived representative time series informed the contributions of the ICs to the observed signal under movie watching conditions.

Temporal variance of the RSN representative time series

We compared the variance of the network representative time series of the PCUN and DMN that were extracted from the regression model, which reflected the fluctuation level of the networks while watching movies. The variance metrics were calculated separately for normal and random movie conditions. Repeated-measure ANOVA was applied to examine the interaction effect between the movie type and networks. We also introduced the mV as a reference to rule out systematic bias in the analysis. This network was the most consistent IC in resting-state scans across subjects, and it covered the primary visual regions. Due to its role in primary visual processing, the mV was expected to reveal no difference in the variance of network representative time series between the two movie conditions.

Functional network connectivity between the PCUN and DMN

We investigated how the two RSNs changed their functional coupling when different movies were watched. The strength of the functional coupling between the PCUN and DMN was measured using the functional network connectivity (FNC). For each subject, we calculated Pearson's correlation coefficient between the network representative time series of the DMN and PCUN obtained from the regression model. The correlation coefficient was then transformed into Fisher's *Z* score to represent the FNC. The FNCs between the PCUN and DMN were compared across the normal and random movie conditions. Besides, we calculated the FNCs between the mV and the two RSNs under the movie-watching conditions. Repeated-measure ANOVA was applied to examine whether the PCUN and DMN are differently involved in visual processing under movie-watching conditions.

Functional connectivity within the DMN and PCUN

To further examine the functional connectivity (FC) within and between RSNs, we parceled the two RSNs into regions of interest (ROIs) and examined the interregional FC. Two steps were implemented to define the ROIs within the RSNs. First, the spatial maps of the three RSNs (DMN, PCUN, mV) obtained in gRAICAR were thresholded at $|Z| > 2$ to identify the core regions. To be consistent with previous studies, we then defined the centers of the ROIs according to the scheme proposed by Power et al. (2011). Those ROIs falling into the thresholded RSN maps were assigned to the corresponding RSNs. Note that the ICA-derived RSN maps contain overlapped regions between the PCUN and DMN, so the ROIs falling into the overlapping regions were excluded from the current ROI analysis. The time series of the ROIs

were obtained by averaging the voxel-wise time series within a sphere surrounding the centers of the ROIs. The radius of the sphere was 6 mm. Pearson's correlation coefficients between the time series were calculated and transformed into Fisher's Z values to measure the FC between the ROIs. With these measures, an inter-ROI FC matrix was computed for each movie condition and subject. This matrix could be separated into several blocks by grouping ROIs into different RSNs. The intranetwork FC and internetwork FC were summarized by averaging the FC values within the corresponding blocks of the FC matrices. The intranetwork and internetwork FC were compared between the normal movie and random movie conditions.

Reliability measures

The reliability of the measures of network representative time series (variance, FNC, and FC) in the normal and random movie conditions was estimated by the interclass correlation coefficient (ICC) (Zuo and Xing 2014; Zuo et al. 2013). More specifically, the network representative time series and ROI time series during the viewing of the movies were temporally split into the first half and the second half in equal length. Next, the above analyses were repeated on both halves, and the ICCs of all measures of interest (the comparison results reported in Figs. 2 and 3) were estimated using a linear-mixed effect modal (Chen et al. 2015) implemented using R (https://www.r-project.org).

Results

Identified RSNs

The ICA decomposed each subject's resting-state fMRI data into ICs. The number of components varied from 30 to 60 across different subjects. The gRAICAR algorithm matched the ICs across subjects and resulted in 35 ACs that linked at least 3 subjects. The first 10 ACs showing the highest inter-subject consistency (all subjects had > 95% confidence) were preserved for the following analysis. The DMN, PCUN, and mV were identified from these 10 ACs. More specifically, mV, DMN and PCUN were identified by gRAICAR as the 2nd, 7th and 3rd ACs, which indicated that they were reliably identified (Yang et al. 2012). Their spatial maps are presented in Fig. 1, which demonstrates the core regions of the DMN: the medial prefrontal cortex, posterior cingulate cortex and lateral parietal cortex; for the PCUN, the main regions are located at the precuneus, mid-cingulate cortex, inferior parietal lobule, and dorsal angular gyrus; for the mV, the main regions are located at the primary visual regions. The locations of the core regions were consistent with those of previous reports (Buckner et al. 2008; Calhoun et al. 2008b; Gilmore et al. 2015; Laird et al. 2011; Raichle 2015; Smith et al. 2013). We calculated the mean inter-subject spatial correlation coefficients for mV, DMN and PCUN. The spatial similarity for mV, DMN and PCUN was 0.39, 0.27 and 0.31, respectively.

Fluctuating representative time series of the PCUN and DMN in movie conditions

As shown in Fig. 2, the variance of the DMN and PCUN network representative time series during the two movie conditions was compared. With the network and movie type as within-subject independent variables, a two-way repeated-measure ANOVA revealed a significant interaction between the network and movie type factors ($F(1, 47) = 8.750$, $p = 0.005$, $\eta^2 = 0.157$), indicating that the contextual information in the movies modulated the variance of the PCUN and DMN in different ways. A post hoc analysis with the Bonferroni correction indicated that while watching the normal movie, the PCUN exhibited a higher variance compared to the DMN ($t = 2.813$, $p < 0.001$), but such a difference was not significant in the random movie condition ($t = -0.492$, $p = 0.471$). The post hoc analysis also indicated that compared to the random movie condition, the PCUN showed a significantly higher variance in the normal movie condition ($t = 2.234$, $p = 0.037$), whereas the DMN showed a trend to respond inversely, which was statistically insignificant ($t = -2.087$, $p = 0.057$). As expected, the mV did not show a significant difference in its representative time series fluctuations ($t = 1.097$, $p = 0.278$).

Functional couplings between the PCUN and DMN

The group-level averaged ROI-wise FC matrices under each movie condition are shown in Fig. 3a, b, with each row or column representing an ROI. The 3 diagonal blocks from left to right represent the intranetwork FCs of the PCUN, DMN, and mV, respectively. The off-diagonal blocks depict the internetwork FCs. The intranetwork FCs were higher overall than the internetwork FCs in both movie conditions. Figure 3c shows the significant difference between the intra network FCs and the internetwork FC in both conditions. The internetwork FC between the DMN and PCUN (inter-DMN–PCUN FC) was much weaker than the intra-DMN FC and intra-PCUN ($p < 0.001$), indicating that there is some extent of functional segregation between the PCUN and DMN. More importantly, the intra-DMN FC did not significantly change between the two movie conditions ($t = 0.658$, $p = 0.514$), whereas the intra-PCUN FC became significantly lower in the random movie condition ($t = 3.969$, $p < 0.001$). In other words, the intra-DMN and intra-PCUN FCs were modulated differently by the movie types, indicating that the

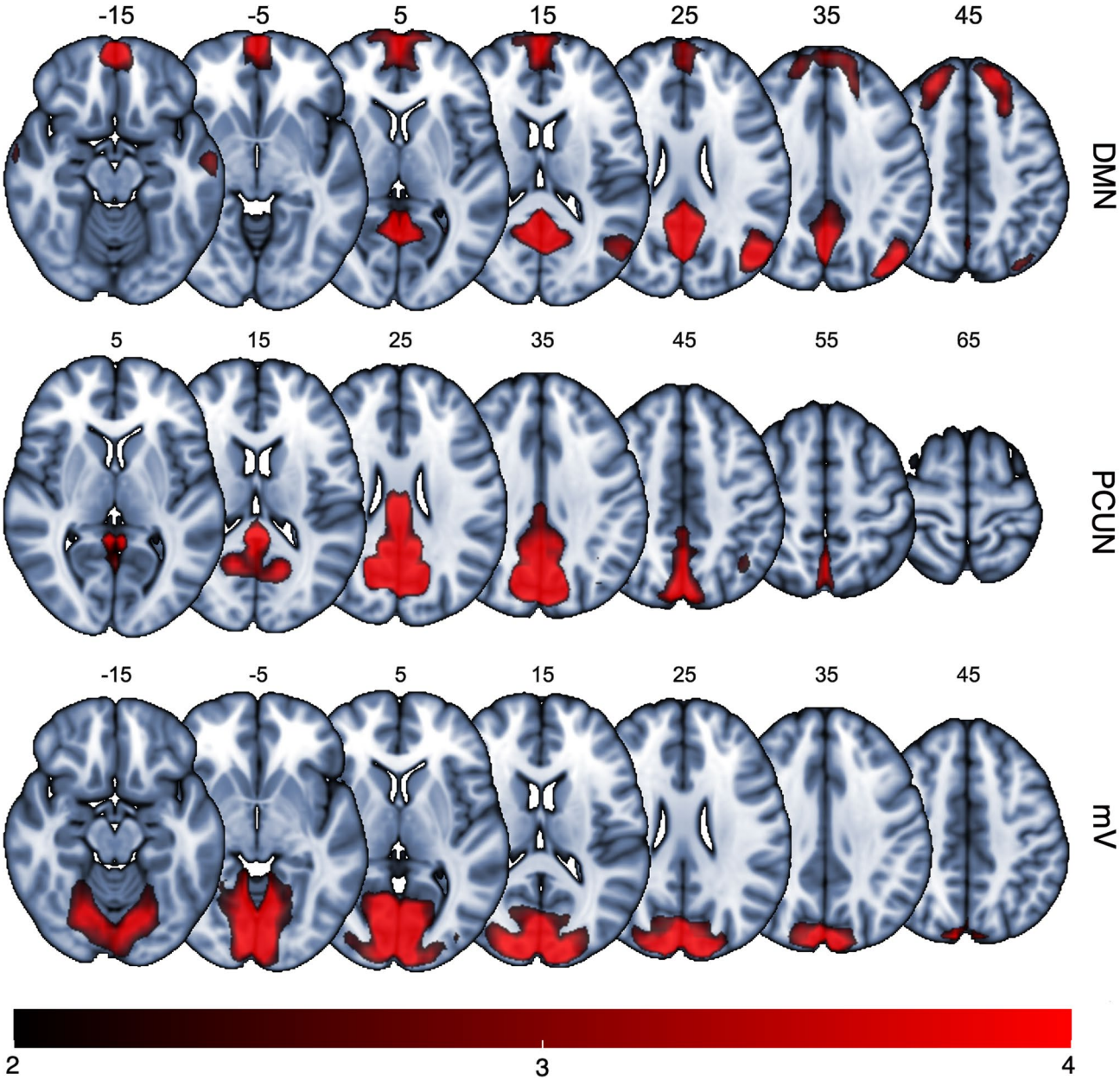

Fig. 1 Spatial maps of the default mode network (DMN), precuneus network (PCUN), and medial visual network (mV) plotted over the Montréal Neurological Institute (MNI) template. The indices above each slice indicate the corresponding coordinates in the inferior–superior direction. Smoothness and thresholding were applied here for better visualization. The colors indicate the contribution of the voxels to the observed independent component. The contribution increases as the color change from dark to red

two RSNs play different functional roles in processing the information in the movies.

The analyses also showed that even though the PCUN ROIs were less functionally connected in the random movie condition, the PCUN intranetwork FC was still significantly higher than the inter-DMN–PCUN FC measured in both movie conditions ($t = 9.280$, $p < 0.001$ for the normal movie; $t = 19.228$, $p < 0.001$ for the random movie), further supporting the functional independence of the PCUN. As a reference network, the intra-mV FC was consistently higher than the internetwork FC (results not shown), which agreed with the consensus that the involvement and functional specificity of the primary visual regions should be strong in movie-watching conditions.

The modulation effects of the movie conditions on the FNC between RSNs are shown in Fig. 3d. The FNC between the PCUN and DMN was significantly modulated by the movie conditions, with a lower FNC in the

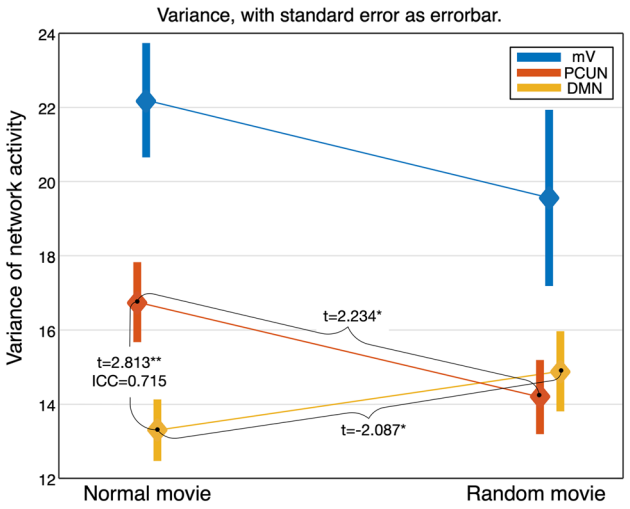

Fig. 2 ANOVA revealed significant interactions between networks (PCUN, red line; DMN, yellow line) and movie conditions (normal and random) on the variance of representative time series fluctuation. The diamond shapes indicate the mean values and the error bars present the standard error metrics. Comparisons showing a significant difference are marked with t values and the significant levels are indicated by the asterisks (*$p<0.05$, **$p<0.01$, ***$p<0.005$). The PCUN and DMN exhibited inverse patterns. The PCUN exhibits a stronger variance of fluctuation in the normal movie condition than in the random movie condition, whereas the DMN shows a significantly lower variance of fluctuation in the normal movie condition. The mV (blue line) is shown here as a reference. As expected, the mV network shows no significant difference between the movie conditions ($t=1.097$, $p=0.278$). The ICCs of the difference in variance between the PCUN and DMN during the normal movie condition and random movie condition are 0.715 and 0.675, respectively, suggesting that the observed difference is reliable

random movie ($t=2.095$, $p=0.042$). This result was consistent with the FC results regarding the decreased inter-DMN–PCUN FC in the random movie condition.

We also compared the intranetwork and internetwork FC when including the overlap regions between PCUN and DMN and calculated the temporal splitting half ICC. The results repeated the patterns discovered when the analysis did not include the overlap regions. The intra-DMN and intra-PCUN FCs were both higher than the inter-DMN–PCUN FC in both conditions. Specifically, in the normal movie condition, the intra-DMN FC and intra-PCUN FC were higher than the inter-DMN–PCUN FC ($t=7.571$, $p<0.001$, ICC = 0.672; $t=14.390$, $p<0.001$, ICC = 0.712, respectively). In the random movie condition, the intra-DMN FC and intra-PCUN FC were also higher than the inter-DMN–PCUN FC ($t=11.066$, $p<0.001$, ICC = 0.485; $t=18.593$, $p<0.001$, ICC = 0.605, respectively).

Functional couplings between the PCUN and mV

Comparing the PCUN-mV FNC and the DMN-mV FNC, a two-way repeated-measure ANOVA found no significant interaction between the network pair and movie type ($F(1,47)=0.048$, $p=0.828$, Fig. 3d, yellow and blue lines). The main effects of both independent variables were significant (network: $F(1,47)=20.357$, $p<0.001$; movie type: $F(1,47)=16.566$, $p<0.001$). The PCUN-mV FNC was significantly higher than the DMN-mV FC in both conditions (normal movie: $t=3.375$, $p<0.01$; random movie: $t=3.740$, $p<0.001$), indicating that compared to the DMN, the PCUN has a stronger functional relevance with mV, and it may play a more important role in the processing of visual materials with continuous contexts.

Reliability of measuring network representative time series

The split-half ICC of the variance of the PCUN, DMN, and mV during the normal movie was 0.673, 0.696, and 0.511, respectively, which was in the range of the fair ($0.40<\text{ICC}<0.59$) to good level ($0.60<\text{ICC}<0.74$); during the random movie, the ICCs were 0.472, 0.695, and 0.462, respectively. The ICC of the variance difference between the PCUN and DMN was 0.715 for the normal movie condition and 0.675 for the random movie condition.

The split-half ICCs of the inter-DMN–PCUN FC, intra-DMN FC, and intra-PCUN FC were 0.678, 0.666, and 0.690, respectively, for the normal movie condition, which were in the range of good reliability. The ICCs while watching the random movie was 0.546, 0.537, and 0.652, respectively, which were in the range of fair to good reliability. Comparing the normal and random movie conditions, the ICCs of the difference in intra-DMN FC, in the intra-PCUN, and in the inter-DMN–PCUN FC were 0.436, 0.524, and 0.489, respectively. Comparing the inter–DMN–PCUN FC in the random movie condition to the intra-PCUN FC, the ICC of the difference was 0.605 for the intra-PCUN in the normal condition and 0.507 for the intra-PCUN in the random condition.

The ICC of the PCUN-mV FNC, DMN-mV FNC, and PCUN–DMN FNC was 0.296, 0.460, and 0.707 for the normal movie, respectively, and 0.721, 0.524, and 0.361 for the random movie. The ICC of the difference between the PCUN-mV FNC and the DMN-mV FNC was 0.459 in the normal movie condition and 0.522 for the random movie condition. The above results indicate that all variances, all FC metrics, and most of the FNC metrics observed in this study have a fair to good reliability.

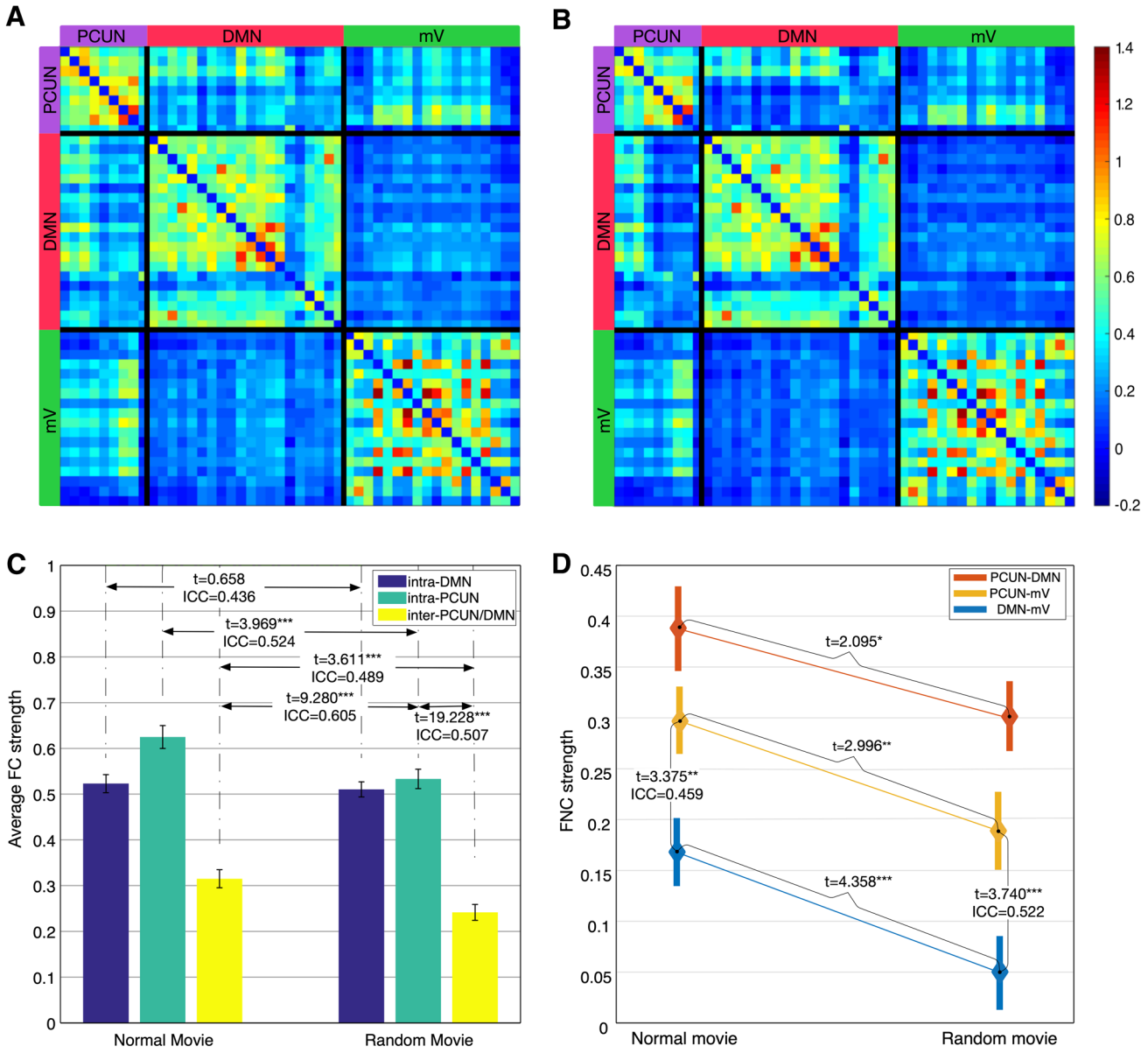

Fig. 3 Functional connectivity comparisons among RSNs and movie conditions. **a**, **b** Present the group-level averaged ROI-wise FC matrices. **a** is for the normal movie condition and **b** is for the random movie condition. In the matrices, colors from dark blue to dark red indicate the strength of FC from negative to positive. The FC matrices are symmetric and contain 3 intranetwork FC blocks (diagonal blocks) and 3 internetwork FC blocks (off-diagonal blocks). In both movie conditions, the intranetwork FC blocks show consistent patterns. However, the internetwork FC blocks appear to be lower while the random movie is watched. The pattern is supported by averaging FC within each block: intra-PCUN, intra-DMN, and inter-DMN–PCUN, as depicted in **c**. **c** Presents statistical comparison results among the FC metrics. In both conditions, all intranetwork FCs are higher than the inter-DMN–PCUN FC. The intra-PCUN FC is more sensitive to movie conditions than the intra-DMN FC. These results indicate the functional independence between the DMN and PCUN. **d** Presents the FNC metrics in the two conditions. The FNC between the PCUN and mV is higher than the functional coupling between the DMN and mV, indicating their different functional roles in processing the visual stimuli. The ICCs of the observed differences are also shown below the corresponding *t* values

Discussion

We adopted natural movies and their storyline-scrambled versions as natural stimuli to investigate the functional segregation between the DMN and PCUN. The main findings are: (1) scrambling the contextual information altered the fluctuation level of the DMN and PCUN in different directions; (2) the functional connectivity within the PCUN showed a significantly higher sensitivity to the continuity of the context compared to the intra-DMN FC; and (3) the

PCUN exhibited a significantly stronger functional network connectivity with the primary visual regions than the DMN. These findings provide evidence for the different functional roles of the PCUN and DMN in the processing of natural stimuli and indicate the functional segregation between the two RSNs.

The functional segregation between the DMN and PCUN in a natural viewing paradigm helps to advance our understanding of the functions of the two networks. Previously, the functional segregation between the DMN and PCUN had only been investigated in the resting state or in repetitive, single-domain cognitive tasks. Evidence from the resting-state functional connectivity studies (Power et al. 2011; Yeo et al. 2011) inferred the functional segregation of the two networks based on patterns of correlations (i.e., the intranetwork FC was higher than the internetwork FC), which does not directly reveal the difference in functional roles between the two RSNs. With a content-rich natural viewing paradigm, our results help to more directly reveal the functional roles of the PCUN. For instance, the continuity of the context modulated the fluctuations of the PCUN and DMN in different directions, and the PCUN was more involved in processing of visual information in an intact natural movie.

On the other hand, studies using single-domain cognitive tasks have demonstrated that the PCUN plays an important role in memory and the detection of novelty (Gur et al. 2007; Kafkas and Montaldi 2014; Lundstrom et al. 2003). However, given that the core region of the PCUN, the precuneus, is widely connected to other regions in the brain (Cunningham et al. 2017; Van Den Heuvel et al. 2009; Zhang and Li 2013) and numerous studies have indicated its involvement in a wide range of cognitive processes (for a review, see Cavanna and Trimble 2006; van den Heuvel and Sporns 2013), the function of the PCUN may not be specific to a single cognitive domain. The roles of the PCUN may be more comprehensively revealed in a content-rich natural viewing paradigm. Echoing this argument, a recent study has classified patients with first-episode psychosis from normal controls based on the response of the PCU when watching a fantasy movie (Rikandi et al. 2017).

The different representative time series patterns of the PCUN and DMN reflect the different mental states of the subjects when viewing the different versions of the movie. The DMN has been related to internal-directed spontaneous thoughts. Its lower fluctuation in the normal movie condition implies that the viewers were watching the movies dedicatedly and relating the stories and characters with themselves. Such mental states were disrupted in the random movie condition. More specifically, scrambling the frames of a movie increased the cognitive load required for understanding the stories. Such an increased cognitive load includes retrieving the memory of the previous frames, comparing the abstract meaning of frames, and making inferences about the stories. Such an externally directed, attention-demanding process might suppress the representative time series of the DMN. On the other hand, the PCUN showed a different representative time series pattern. The finding that the PCUN exhibited a higher variance in representative time series in the normal movie condition and a lower variance during the random movie could be explained by the proposal that the PCUN is related to the memory and perceiving of novelty (Gilmore et al. 2015). The stories were presented successively in the normal movie, and only some of the scenes required subjects to retrieve memory about the previous scenes and to make an inference about the stories (which may be termed complex scenes). The PCUN was lower activated during the successive scenes and higher activated during the complex scenes. Switching between the higher and lower activating level resulted in the higher variance during the random movie. In contrast, the PCUN would be more consistently activated during the random movie due to the need for more frequently and actively retrieving memory and making inferences. Furthermore, PCUN and DMN demonstrated a difference in the involvement of visual processing. The functional coupling between the PCUN and mV was higher than that between the DMN and mV in both movie conditions (Fig. 3d, blue and yellow lines), indicating that the PCUN may have a closer functional role to the visual process of natural stimuli.

Furthermore, since there is no gold standard for justifying the biological meanings of the networks only using resting-data, the existing parcellation schemes of RSNs have not achieved a consensus due to their differences in algorithms and criteria. This paradigm provides an avenue to examine the functional roles of RSNs in a real-life context and helps to infer whether and in what context the resting-state networks play different functional roles.

To rule out potential bias in the methodology, we included the mV network as a reference and examined the reliability of the measures (variance, FNC, and FC). Because the random movie was different from the normal movie only in the continuity of the context, we expected that the mV would not significantly change either in the fluctuation level or in the intramV FC. As expected, the unchanged fluctuation level and the intranetwork FC of mV between the two movie conditions indicate that the comparisons and methodology are unbiased. The ICC results indicate that the reliability of the analysis ranged from fair to good in all variances and FC metrics, supporting the reliability of the results.

Limitation and prospect

The current study provides evidence for the functional segregation of the DMN and PCUN in natural movie conditions. However, how the integrity degree of natural stimuli modulates the segregation requires further research that includes

behavioral tests and finely tuned stimuli. On the other hand, the relation between the representative time series of RSNs and the contextual information of natural stimuli indicates that RSNs may provide clues for decoding information from RSN representative time series. However, which specific characteristics of the content in the movie would enhance or alleviate the difference between the PCUN and DMN still require further study.

Conclusion

To conclude, the distinct patterns of the PCUN and DMN representative time series and the separation in functional connectivity under natural stimuli suggest that the DMN and PCUN are two functionally segregated networks during real-life information processing.

Funding This study is supported by Grants from the National Science Foundation of China (Grant numbers: 81270023, 81571756, 81971682 to Z.Y., 81471740 to X.-N.Z.), the National Key R&D Program of China (Grant No.: 2018YFC2001600 to Z.Y.), the Beijing Nova Program for Science and Technology (XXJH2015B079 to Z.Y.), Shanghai Municipal Education Commission—Gaofeng Clinical Medicine Grant Support (Grant No. 20171929 to Z.Y.), Hundred-Talent Fund from Shanghai Municipal Commission of Health (Grant No. 2018BR17 to Z.Y.]), Research Fund from Shanghai Mental Health Center (13dz2260500 to Z.Y.), Beijing Municipal Science and Tech Commission (Z161100002616023, Z171100000117012 to X.-N.Z.), and the National Basic Research Program (973 Program: 2015CB351702 to X.-N.Z.).

Compliance with ethical standards

Conflict of interest The authors declare that they have no conflict of interest.

Research involving human participants and/or animals All procedures performed in studies involving human participants were in accordance with the ethical standards of the institutional and/or national research committee and with the 1964 Helsinki declaration and its later amendments or comparable ethical standards. This article does not contain any studies with animals performed by any of the authors.

Informed consent Informed consent was obtained from all individual participants included in the study.

References

Andrews-Hanna JR, Reidler JS, Huang C, Buckner RL (2010) Evidence for the default network's role in spontaneous cognition. J Neurophysiol 104(1):322–335. https://doi.org/10.1152/jn.00830.2009

Avants BB, Tustison NJ, Song G, Cook PA, Klein A, Gee JC (2011) A reproducible evaluation of ANTs similarity metric performance in brain image registration. NeuroImage 54(3):2033–2044. https://doi.org/10.1016/j.neuroimage.2010.09.025

Beckmann CF, Smith SM (2004) Probabilistic independent component analysis for functional magnetic resonance imaging. IEEE Trans Med Imaging 23(2):137–152. https://doi.org/10.1109/TMI.2003.822821

Beckmann C, Mackay C, Filippini N, Smith S (2009) Group comparison of resting-state FMRI data using multi-subject ICA and dual regression. NeuroImage 47:S148. https://doi.org/10.1016/S1053-8119(09)71511-3

Biswal B, Yetkin FZ, Haughton VM, Hyde JS (1995) Functional connectivity in the motor cortex of resting human brain using echo-planar MRI. Magn Reson Med 34(4):537–541. https://doi.org/10.1002/mrm.1910340409

Buckner RL, Andrews-Hanna JR, Schacter DL (2008) The brain's default network: anatomy, function, and relevance to disease. Ann N Y Acad Sci 1124:1–38. https://doi.org/10.1196/annals.1440.011

Calhoun VD, Kiehl KA, Pearlson GD (2008a) Modulation of temporally coherent brain networks estimated using ICA at rest and during cognitive tasks. Hum Brain Mapp 29(7):828–838. https://doi.org/10.1002/hbm.20581

Calhoun VD, Maciejewski PK, Pearlson GD, Kiehl KA (2008b) Temporal lobe and "default" hemodynamic brain modes discriminate between schizophrenia and bipolar disorder. Hum Brain Mapp 29(11):1265–1275. https://doi.org/10.1002/hbm.20463

Cavanna AE, Trimble MR (2006) The precuneus: a review of its functional anatomy and behavioural correlates. Brain 129(3):564–583. https://doi.org/10.1093/brain/awl004

Chen B, Xu T, Zhou C, Wang L, Yang N, Wang Z et al (2015) Individual variability and test-retest reliability revealed by ten repeated resting-state brain scans over one month. PLoS One 10(12):1–21. https://doi.org/10.1371/journal.pone.0144963

Chen H-Y, Gilmore AW, Nelson SM, McDermott KB (2017) Are there multiple kinds of episodic memory? An fMRI investigation comparing autobiographical and recognition memory tasks. J Neurosci 37(10):2764–2775. https://doi.org/10.1523/JNEUROSCI.1534-16.2017

Cunningham SI, Tomasi D, Volkow ND (2017) Structural and functional connectivity of the precuneus and thalamus to the default mode network. Hum Brain Mapp 38(2):938–956. https://doi.org/10.1002/hbm.23429

Fischl B (2012) FreeSurfer. NeuroImage 62(2):774–781. https://doi.org/10.1016/j.neuroimage.2012.01.021

Fox MD, Snyder AZ, Vincent JL, Corbetta M, Van Essen DC, Raichle ME (2005) From the Cover: the human brain is intrinsically organized into dynamic, anticorrelated functional networks. Proc Natl Acad Sci 102(27):9673–9678. https://doi.org/10.1073/pnas.0504136102

Gilmore AW, Nelson SM, McDermott KB (2015) A parietal memory network revealed by multiple MRI methods. Trends Cogn Sci 19(9):534–543. https://doi.org/10.1016/j.tics.2015.07.004

Gilmore AW, Kalinowski SE, Milleville SC, Gotts SJ, Martin A (2019) Identifying task-general effects of stimulus familiarity in the parietal memory network. Neuropsychologia 124:31–43. https://doi.org/10.1016/j.neuropsychologia.2018.12.023

Golland Y, Bentin S, Gelbard H, Benjamini Y, Heller R, Nir Y et al (2007) Extrinsic and intrinsic systems in the posterior cortex of the human brain revealed during natural sensory stimulation. Cereb Cortex 17(4):766–777. https://doi.org/10.1093/cercor/bhk030

Greicius MD, Srivastava G, Reiss AL, Menon V (2004) Default-mode network activity distinguishes Alzheimer's disease from healthy aging: evidence from functional MRI. Proc Natl Acad Sci USA 101(13):4637–4642. https://doi.org/10.1073/pnas.0308627101

Gur RC, Turetsky BI, Loughead J, Waxman J, Snyder W, Ragland JD et al (2007) Hemodynamic responses in neural circuitries for detection of visual target and novelty: an event-related fMRI

study. Hum Brain Mapp 28(4):263–274. https://doi.org/10.1002/hbm.20319
Hasson U, Nir Y, Levy I, Fuhrmann G, Malach R (2004) Intersubject synchronization of cortical activity duringnatural vision. Science 303(5664):1634–1640. https://doi.org/10.1126/science.1089506
Hu Y, Wang J, Li C, Wang YS, Yang Z, Zuo XN (2016) Segregation between the parietal memory network and the default mode network: effects of spatial smoothing and model order in ICA. Sci Bull 61(24):1844–1854. https://doi.org/10.1007/s11434-016-1202-z
Huth AG, de Heer WA, Griffiths TL, Theunissen FE, Gallant JL (2016) Natural speech reveals the semantic maps that tile human cerebral cortex. Nature 532(7600):453–458. https://doi.org/10.1038/nature17637
Jones DT, Knopman DS, Gunter JL, Graff-Radford J, Vemuri P, Boeve BF et al (2016) Cascading network failure across the Alzheimer's disease spectrum. Brain 139(2):547–562. https://doi.org/10.1093/brain/awv338
Kafkas A, Montaldi D (2014) Two separate, but interacting, neural systems for familiarity and novelty detection: a dual-route mechanism. Hippocampus 24(5):516–527. https://doi.org/10.1002/hipo.22241
Laird AR, Fox PM, Eickhoff SB, Turner JA, Ray KL, McKay DR et al (2011) Behavioral interpretations of intrinsic connectivity networks. J Cogn Neurosci 23(12):4022–4037. https://doi.org/10.1162/jocn_a_00077
Lankinen K, Saari J, Hari R, Koskinen M (2014) Intersubject consistency of cortical MEG signals during movie viewing. NeuroImage 92:217–224. https://doi.org/10.1016/j.neuroimage.2014.02.004
Lundstrom BN, Petersson KM, Andersson J, Johansson M, Fransson P, Ingvar M (2003) Isolating the retrieval of imagined pictures during episodic memory: activation of the left precuneus and left prefrontal cortex. NeuroImage 20(4):1934–1943. https://doi.org/10.1016/j.neuroimage.2003.07.017
Manjón JV, Coupé P (2016) volBrain: an online MRI brain volumetry system. Front Neuroinform 10(July):1–14. https://doi.org/10.3389/fninf.2016.00030
Manoliu A, Riedl V, Zherdin A, Mühlau M, Schwerthöffer D, Scherr M et al (2014) Aberrant dependence of default mode/central executive network interactions on anterior insular salience network activity in schizophrenia. Schizophr Bull 40(2):428–437. https://doi.org/10.1093/schbul/sbt037
McDermott KB, Gilmore AW, Nelson SM, Watson JM, Ojemann JG (2017) The parietal memory network activates similarly for true and associative false recognition elicited via the DRM procedure. Cortex 87:96–107. https://doi.org/10.1016/j.cortex.2016.09.008
Menon V (2011) Large-scale brain networks and psychopathology: a unifying triple network model. Trends Cogn Sci 15(10):483–506. https://doi.org/10.1016/j.tics.2011.08.003
Padmanabhan A, Lynch CJ, Schaer M, Menon V (2017) The default mode network in autism. Biol Psychiatry Cogn Neurosci Neuroimaging 2(6):476–486. https://doi.org/10.1016/j.bpsc.2017.04.004
Peelen MV, Fei-Fei L, Kastner S (2009) Neural mechanisms of rapid natural scene categorization in human visual cortex. Nature 460(7251):94–97. https://doi.org/10.1038/nature08103
Power JD, Cohen AL, Nelson SM, Wig GS, Barnes KA, Church JA et al (2011) Functional network organization of the human brain. Neuron 72(4):665–678. https://doi.org/10.1016/j.neuron.2011.09.006
Raichle ME (2015) The brain's default mode network. Annu Rev Neurosci 38(1):433–447. https://doi.org/10.1146/annurev-neuro-071013-014030
Rikandi E, Pamilo S, Mäntylä T, Suvisaari J, Kieseppä T, Hari R et al (2017) Precuneus functioning differentiates first-episode psychosis patients during the fantasy movie Alice in Wonderland. Psychol Med 47(3):495–506. https://doi.org/10.1017/S0033291716002609
Shirer WR, Ryali S, Rykhlevskaia E, Menon V, Greicius MD (2012) Decoding subject-driven cognitive states with whole-brain connectivity patterns. Cereb Cortex 22(1):158–165. https://doi.org/10.1093/cercor/bhr099
Simony E, Honey CJ, Chen J, Lositsky O, Yeshurun Y, Wiesel A, Hasson U (2016) Dynamic reconfiguration of the default mode network during narrative comprehension. Nat Commun 7(July):12141. https://doi.org/10.1038/ncomms12141
Smith SM, Fox PT, Miller KL, Glahn DC, Fox PM, Mackay CE et al (2009) Correspondence of the brain's functional architecture during activation and rest. Proc Natl Acad Sci 106(31):13040–13045. https://doi.org/10.1073/pnas.0905267106
Smith Stephen M, Beckmann CF, Andersson J, Auerbach EJ, Bijsterbosch J, Douaud G et al (2013) Resting-state fMRI in the human connectome project. NeuroImage 80:144–168. https://doi.org/10.1016/j.neuroimage.2013.05.039
van den Heuvel MP, Sporns O (2013) Network hubs in the human brain. Trends Cogn Sci 17(12):683–696. https://doi.org/10.1016/j.tics.2013.09.012
van den Heuvel MP, Mandl RCW, Kahn RS, Hulshoff Pol HE (2009) Functionally linked resting-state networks reflect the underlying structural connectivity architecture of the human brain. Hum Brain Mapp 30(10):3127–3141. https://doi.org/10.1002/hbm.20737
Vanderwal T, Kelly C, Eilbott J, Mayes LC, Castellanos FX (2015) Inscapes: a movie paradigm to improve compliance in functional magnetic resonance imaging. NeuroImage 122:222–232. https://doi.org/10.1016/j.neuroimage.2015.07.069
Vanderwal T, Eilbott J, Finn ES, Craddock RC, Turnbull A, Castellanos FX (2017) Individual differences in functional connectivity during naturalistic viewing conditions. NeuroImage 157(April):521–530. https://doi.org/10.1016/j.neuroimage.2017.06.027
Wilson SM, Molnar-Szakacs I, Iacoboni M (2008) Beyond superior temporal cortex: intersubject correlations in narrative speech comprehension. Cereb Cortex 18(1):230–242. https://doi.org/10.1093/cercor/bhm049
Xu T, Yang Z, Jiang L, Xing XX, Zuo XN (2015) A connectome computation system for discovery science of brain. Sci Bull 60(1):86–95. https://doi.org/10.1007/s11434-014-0698-3
Yang Z, LaConte S, Weng X, Hu X (2008) Ranking and averaging independent component analysis by reproducibility (RAICAR). Hum Brain Mapp 29(6):711–725. https://doi.org/10.1002/hbm.20432
Yang Z, Zuo XN, Wang P, Li Z, LaConte SM, Bandettini PA, Hu XP (2012) Generalized RAICAR: discover homogeneous subject (sub)groups by reproducibility of their intrinsic connectivity networks. NeuroImage 63(1):403–414. https://doi.org/10.1016/j.neuroimage.2012.06.060
Yang Z, Chang C, Xu T, Jiang L, Handwerker DA, Castellanos FX et al (2014) Connectivity trajectory across lifespan differentiates the precuneus from the default network. NeuroImage 89:45–56. https://doi.org/10.1016/j.neuroimage.2013.10.039
Yeo BTT, Krienen FM, Sepulcre J, Sabuncu MR, Lashkari D, Hollinshead M et al (2011) The organization of the human cerebral cortex estimated by intrinsic functional connectivity. J Neurophysiol 106:1125–1165. https://doi.org/10.1152/jn.00338.2011
Zhang S, Li C-SR (2013) Functional connectivity mapping of the human precuneus by resting state fMRI. NeuroImage 59(4):3548–3562. https://doi.org/10.1016/j.neuroimage.2011.11.023.Functional

Zuo XN, Xing XX (2014) Test-retest reliabilities of resting-state FMRI measurements in human brain functional connectomics: a systems neuroscience perspective. Neurosci Biobehav Rev 45:100–118. https://doi.org/10.1016/j.neubiorev.2014.05.009

Zuo XN, Kelly C, Adelstein JS, Klein DF, Castellanos FX, Milham MP (2010) Reliable intrinsic connectivity networks: test-retest evaluation using ICA and dual regression approach. NeuroImage 49(3):2163–2177. https://doi.org/10.1016/j.neuroimage.2009.10.080

Zuo XN, Xu T, Jiang L, Yang Z, Cao XY, He Y et al (2013) Toward reliable characterization of functional homogeneity in the human brain: preprocessing, scan duration, imaging resolution and computational space. NeuroImage 65:374–386. https://doi.org/10.1016/j.neuroimage.2012.10.017